PHYSICAL REVIEW B **91**, 020103(R) (2015)

Locally resonant band gaps in periodic beam lattices by tuning connectivity

Pai Wang,[1] Filippo Casadei,[1] Sung Hoon Kang,[1,2,3] and Katia Bertoldi[1,4,*]

[1]*School of Engineering and Applied Sciences, Harvard University, Cambridge, Massachusetts 02138, USA*
[2]*Department of Mechanical Engineering, Johns Hopkins University, Baltimore, Maryland 21218, USA*
[3]*Hopkins Extreme Materials Institute, Johns Hopkins University, Baltimore, Maryland 21218, USA*
[4]*Kavli Institute, Harvard University, Cambridge, Massachusetts 02138, USA*

(Received 12 August 2014; revised manuscript received 5 November 2014; published 26 January 2015)

Lattice structures have long fascinated physicists and engineers not only because of their outstanding functionalities, but also for their ability to control the propagation of elastic waves. While the study of the relation between the connectivity of these systems and their static properties has a long history that goes back to Maxwell, rules that connect the dynamic response to the network topology have not been established. Here, we demonstrate that by tuning the average connectivity of a beam network ($\bar{z}$), locally resonant band gaps can be generated in the structures without embedding additional resonating units. In particular, a critical threshold for $\bar{z}$ is identified, far from which the band gap size is purely dictated by the global lattice topology. By contrast, near this critical value, the detailed local geometry of the lattice also has strong effects. Moreover, in stark contrast to the static case, we find that the nature of the joints is irrelevant to the dynamic response of the lattices. Our results not only shed new light on the rich dynamic properties of periodic lattices, but also outline a new strategy to manipulate mechanical waves in elastic systems.

DOI: 10.1103/PhysRevB.91.020103 PACS number(s): 46.70.De, 46.40.Cd, 62.30.+d

The topology of structures comprising an interconnected network of elastic beams can be effectively described by the coordination number ($\bar{z}$), which is defined as the average number of connections at joints. From a static point of view, reducing $\bar{z}$ makes the structure less rigid until a critical threshold is reached, below which deformation modes of zero energy emerge [1–5]. A global stability criterion that purely depends on $\bar{z}$ was first determined by Maxwell for pin-joined lattices comprising springlike ligaments [1], and then modified to account for the nature (pin or welded) of the joints [6], the bending stiffness of the struts [7,8], self-stresses [9], dislocation defects [10], collapse mechanisms [11], and boundary modes [12–15]. In recent years, the dynamic response of periodic lattices has also attracted considerable interest [16–19] because of their ability to tailor the propagation of elastic waves through directional transmissions [20–23] and band gaps (frequency ranges of strong wave attenuation) [21–24]. Though several studies have shown that the wave propagation properties of periodic lattices are highly sensitive to the architecture of the network [20–24], a global criterion connecting the frequency and size of band gaps to the lattice topology is still not yet in place.

In this Rapid Communication, we study the effects of both the global coordination number ($\bar{z}$) and the local geometric features of periodic networks made of slender beams with finite bending stiffness on the propagation of elastic waves. We consider two-dimensional periodic lattices made of Euler-Bernoulli beams supporting both bending and axial deformations. Each beam is made of a linear elastic isotropic material, has length L, mass per unit length m, bending stiffness EI, axial stiffness EA, and is characterized by a slenderness ratio $\lambda = L\sqrt{EA/(EI)} = 20$. However, it is important to note that all results presented in the Rapid Communication are not affected by this specific choice of λ and that identical findings can be obtained for a network of beams characterized by any value of $\lambda > 10$. To study the propagation of small amplitude elastic waves in such lattices, we perform frequency-domain wave propagation analysis [26,27] within the finite element (FE) framework using the commercial package ABAQUS/STANDARD and Bloch-type boundary conditions are applied to the edges of the unit cell. We then solve the frequency-domain wave equation for wave vectors in the *Brillouin zone* using a perturbation method [25].

We start by investigating the propagation of elastic waves in the triangular lattice (characterized by connectivity $\bar{z} = 6$) with both pin and welded joints. Figures 1(a) and 1(b) show the band structures in terms of the normalized frequency $\omega/\omega_{\text{welded}}$ and $\omega/\omega_{\text{pin}}$, where $\omega_{\text{welded}} = 22.4\sqrt{EI/(mL^4)}$ and $\omega_{\text{pin}} = \pi^2\sqrt{EI/(mL^4)}$ are the first natural frequency of the single beam with both ends fixed (welded) and free to rotate (pin), respectively. As previously predicted [21], the dispersion relations indicate that the structure is characterized by a band gap. However, while such band gap is believed to be due to Bragg scattering, our analysis surprisingly indicates that it is generated by localized resonance, a fact that has not been clearly pointed out before. This important observation is clearly supported by the fact that, regardless of the type of joints, the band at the lower edge of the band gap is completely flat [see red lines in Figs. 1(a) and 1(b)] and located in correspondence of the first natural frequency of the beams (i.e., $\omega/\omega_{\text{welded}} = 1$ and $\omega/\omega_{\text{pin}} = 1$). Furthermore, the Bloch mode shapes of the flat band at the high-symmetry points G, X, and M reported in Figs. 1(c) and 1(d) confirm that each beam vibrates independently according to its natural mode. As a result, the vibration energy is localized by the single-beam resonant mode, preventing the propagation of the elastic waves. In previous studies, the local resonance mechanism was typically realized in heterogeneous systems comprising

*Corresponding author: bertoldi@seas.harvard.edu

 ©2015 American Physical Society

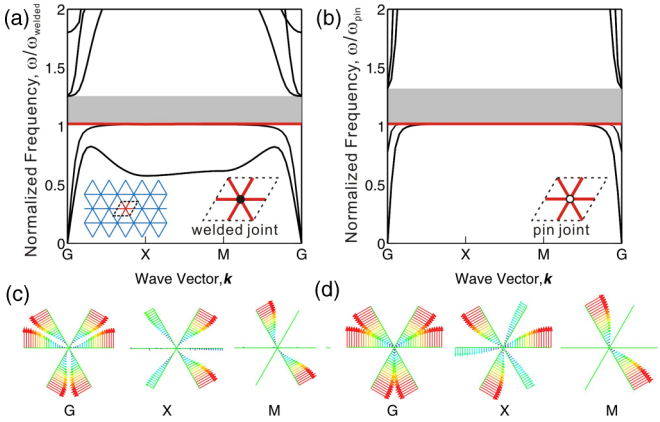

FIG. 1. (Color online) Band structures of triangular periodic beam lattices. (a) Dispersion relation of the triangular lattice with welded joints. (b) Dispersion relation of the triangular lattice with pin joints. The lattice and unit cells with both welded and pin joints are shown as insets. Band gaps are shown as gray-shaded areas and the flat bands at their lower edge are highlighted in red. The Bloch modes of the flat band (the third mode) at high symmetry points of the *Brillouin zone* (G, X, and M) [25] are shown in (c) and (d) for the case of welded and pin joints, respectively. A plot presenting both band structures normalized by the same factor is included in the Supplemental Material [25].

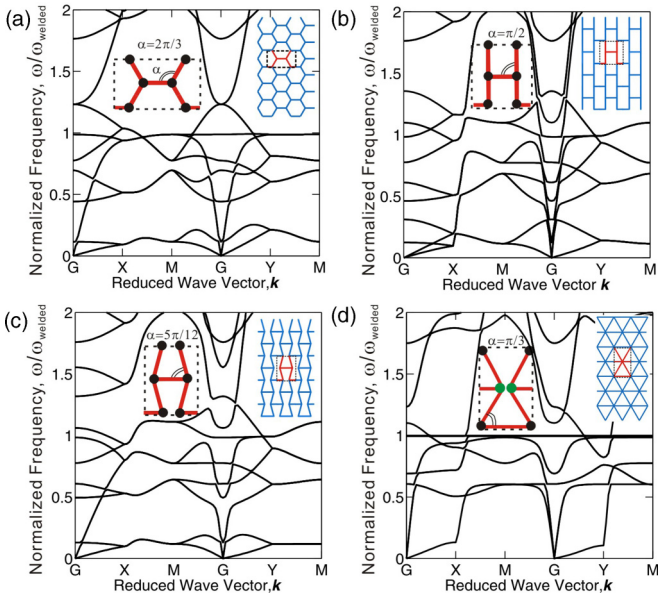

FIG. 2. (Color online) Band structure of periodic lattices with $\bar{z} = 3$ and welded joints. (a) Hexagonal lattice ($\alpha = 2\pi/3$); (b) topologically equivalent lattice with $\alpha = \pi/2$; (c) topologically equivalent lattice with $\alpha = 5\pi/12$; and (d) topologically equivalent lattice with $\alpha = \pi/3$. The lattice structures and unit cells used in the calculations are shown as insets. Note that for $\alpha = \pi/3$ the arrangement of the beams is the same as for the triangular lattice, but the connectivity is still $\bar{z} = 3$. In fact, although for clarity the green-colored joints are drawn separately in the unit cell of (d), they are positioned at the same spatial location. No locally resonant band gap is found for any of the configurations. Results for the same lattices with pin joints are provided in the Supplemental Material [25].

two [27–29], three [30–32], or four [33] different constituent materials. Remarkably, in periodic triangular lattices, even with a single material and building block, local resonances can be exploited to generate band gaps, providing a foundation for the design of a new class of systems to manipulate the propagation of elastic waves. Furthermore, our results also demonstrate that, in order to attenuate the propagation of elastic waves through localized resonances, it is not necessary to embed additional resonating components [23,24,34–42] within the beam lattices. Such single-building-block and single-material system with locally resonant band gap has been previously realized in a one-dimensional setup only [43].

Having demonstrated that the triangular beam lattice is characterized by a locally resonant band gap regardless of the type of joints, we now investigate the dynamic response of the hexagonal lattice, which has the same lattice symmetries of the triangular lattice but a much smaller coordination number (i.e., $\bar{z} = 3$). As shown in Fig. 2(a), the hexagonal lattice with welded joints also exhibits an almost flat band at the resonant frequency of the beams (i.e., $\omega = \omega_{\text{welded}}$). However, in this case the flatband resonant mode does not open a band gap regardless of the types of joints (identical behavior is found in the case of pin joints [25]). By comparing to the triangular lattice, we note that the absence of the locally resonant band gap in the hexagonal lattice could arise either because of the low connectivity number $\bar{z}$ or the different angle α between connected beams. To further inspect the contribution of the latter factor, by keeping $\bar{z} = 3$ and varying α from $2\pi/3$ to $\pi/3$, we construct periodic lattices that are topologically equivalent to the hexagonal lattice and study their dynamic response. As clearly shown in Figs. 2(b)–2(d), though the phononic band structure evolves significantly as α changes, no band gap is observed. It is especially important to note that for $\alpha = \pi/3$ the beams are arranged exactly as in the triangular lattice. However, the network topology is different, as only three, instead of six, beams connect to each other at each joint [see inset in Fig. 2(d)]. Thus, these results conclusively show that the global topology of the network described by the coordination number plays a crucial role in determining the existence of locally resonant band gaps. In addition, our analysis indicates that this conclusion is not affected by the nature of the joints (additional results for pin joints are included in the Supplemental Material [25]).

Next, to further demonstrate the role of the coordination number on the formation of locally resonant band gaps, we investigate a number of periodic beam lattices with $3 < \bar{z} < 6$, as shown in Fig. 3(a). These hybrid lattices are generated by considering enlarged unit cells of the triangular lattice and randomly removing a number of joints and all beams attached to them. Alternatively, lattices with $\bar{z}$ close to 3 are constructed starting with an enlarged unit cell of the hexagonal lattice and filling some randomly chosen hexagons with six triangles. For each value of $\bar{z}$ multiple configurations are analyzed and, since these periodic lattices do not share the same spatial symmetry of the triangular and hexagonal lattices, additional Bloch vectors are considered to determine the presence of band gaps [25]. The results are summarized in Fig. 3(b), where the width of the band gap $\Delta\omega$ is reported for different hybrid lattices with $3 < \bar{z} < 6$. Each circular

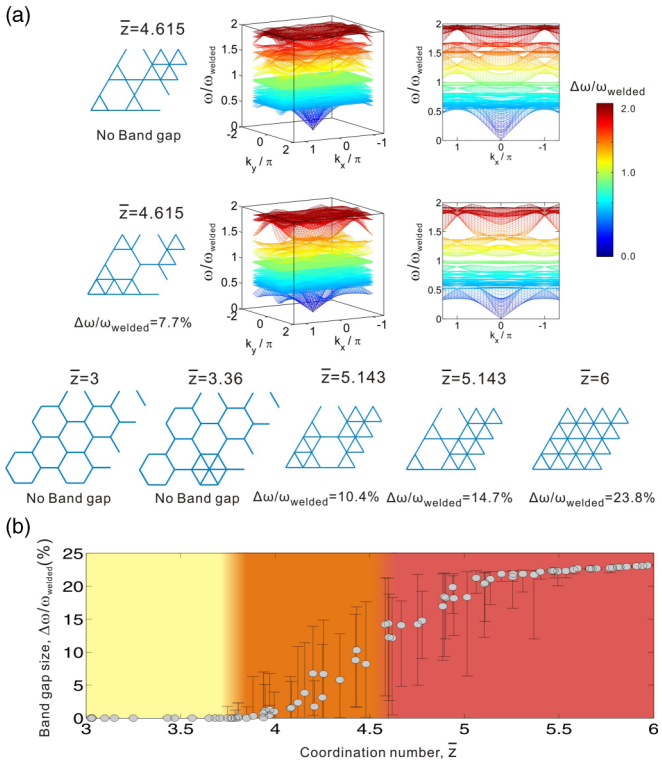

FIG. 3. (Color online) Dynamic response of periodic lattices with $3 < \bar{z} < 6$. (a) Representative unit cells constructed either starting from the triangular lattice and removing a number of randomly chosen nodes or starting from the hexagonal lattice and filling a number of randomly chosen hexagons with six triangles. For two unit cells with $\bar{z} = 4.615$ the band structures are also shown. (b) Relation between normalized average band gap size $\Delta\omega/\omega_{\text{welded}}$ and coordination number $\bar{z}$. The band gap size is computed as the difference between the upper and lower edges of the gap. The error bar at each data point indicates the band gap range of frequencies spanned by all different configurations characterized by the same value of $\bar{z}$.

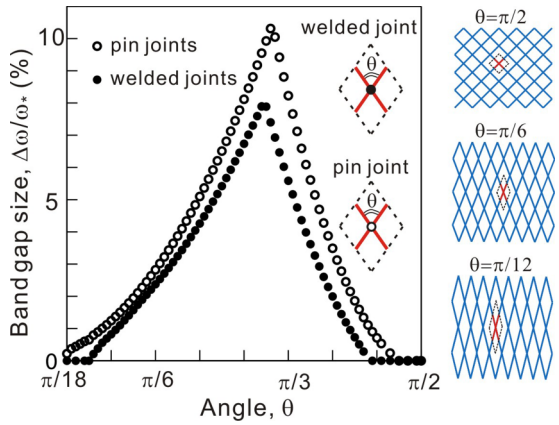

FIG. 4. (Color online) Normalized band gap width $\Delta\omega/\omega_*$ for rhombic lattices that are topologically equivalent to the square lattice. The lattice structures and joint types used in the calculations are shown as insets. The results for lattices with both welded and pin joints are reported. Note that $\omega_* = \omega_{\text{welded}}$ and $\omega_* = \omega_{\text{pin}}$ for lattices with welded and pin joints, respectively.

marker in the plot represents the average band gap width of all configurations considered for that particular value of $\bar{z}$, while the corresponding error bar spans the range of observed $\Delta\omega$. Interestingly, for lattices with low connectivity [i.e., $3.0 < \bar{z} < 3.7$—yellow region in Fig. 3(b)], no locally resonant band gap is observed at $\omega = \omega_{\text{welded}}$.

In contrast, when $4.6 < \bar{z} < 6.0$ [red region in Fig. 3(b)], all considered lattices possess a locally resonant band gap. In particular, for structures with a very high average connectivity (i.e., $\bar{z} > 5.5$), the band gap width $\Delta\omega$ is linearly correlated to the coordination number $\bar{z}$. On the other hand, if $4.6 < \bar{z} < 5.7$, although a locally resonant band gap always exists, its size is not solely determined by $\bar{z}$, but also affected by the specific arrangement of the beams within the unit cell. Finally, when $3.7 < \bar{z} < 4.6$ [orange region in Fig. 3(b)], depending on the local geometric features, the lattice may either have or not have a locally resonant band gap [25].

The results presented in Fig. 3 not only confirm that the global topology of the lattice is the leading factor in determining the existence of a locally resonant band gap, but also indicate that for an intermediate range of $\bar{z}$ the detailed geometry of the lattice plays an important role. To further understand the effect of the arrangement of the beams in lattices characterized by intermediate values of $\bar{z}$, we also study rhombic lattices with $\bar{z} = 4$ and investigate the effect of the angle θ between the beams at the joints. We start from the case of $\theta = \pi/2$, the well-known square lattice, which does not have a locally resonant band gap [21]. However, as shown in Fig. 4, when the angle θ is progressively reduced, a locally resonant band gap appears for rhombic lattices. Interestingly, we also find that a maximum band gap width is achieved for $\theta = 56\pi/180$, regardless of the joint types. Therefore, our results indicate that, when extended to the dynamic response of the beam lattices, Maxwell's rule can be relaxed. In fact, while $\bar{z} = 4$ represents the critical threshold below which a lattice made of springlike ligaments becomes unstable, the rhombic lattices at the threshold can still possess a locally resonant band gap by carefully choosing the angle θ.

In summary, we have numerically investigated the dynamic response of periodic beam lattices. We have found that, in highly connected lattices, the beams themselves act as mechanical resonators, enabling the generation of locally resonant band gaps. Similar to the observation reported for the effective static properties of lattices [1,5,6,8,13,14], our results indicate that the presence and width of the locally resonant band gap depends on the coordination number (i.e., average lattice connectivity, $\bar{z}$). A reduction of $\bar{z}$ results in a decrease of the bandwidth, until a critical threshold is reached, below which the band gap completely closes. On the other hand, we have found that, different from the ground state static properties [6,7,44], the dynamic response of the system is not sensitive to the type of joints. Under dynamic loading, the lattices are in an excited state characterized by a finite level of energy, and the response is not qualitatively affected by the bending stiffness of the joints. Moreover, we have also shown that the average connectivity is not enough to predict the dynamic characteristics of a system when $\bar{z}$ is near the critical threshold. In fact, we identified a transition region where the dynamic

response of the lattices is sensitive to the detailed architecture of the network. Our work paves the way towards the design of a new class of systems made of identical elastic beams that can effectively attenuate the propagation of elastic waves at low frequencies by exploiting local resonances. As an example, highly connected periodic lattices with beam length $\sim$40 mm, thickness $\sim$2.0 mm, which are made of an acrylic polymer that can be easily 3D-printed (Youngs modulus $\sim$1.14 GPa, density $\sim$1050 kg/m^3), exhibit a locally resonant band gap in the audible frequency range (i.e., at around 590 Hz and 1340 Hz for the case of pin and welded joints, respectively).

This work has been supported by Harvard MRSEC through Grant No. DMR-1420570 and by NSF through Grants No. CMMI-1120724 and No. CMMI-1149456 (CAREER). K.B. acknowledges start-up funds from the Harvard School of Engineering and Applied Sciences and the support of the Kavli Institute and Wyss Institute at Harvard University.

[1] J. C. Maxwell, Philos. Mag. Ser. 4 **27**, 294 (1864).
[2] S. Alexander, Phys. Rep. **296**, 65 (1998).
[3] C. S. O'Hern, L. E. Silbert, A. J. Liu, and S. R. Nagel, Phys. Rev. E **68**, 011306 (2003).
[4] M. Wyart, Ann. Phys. (Paris, Fr.) **30**, 1 (2005).
[5] X. Mao, N. Xu, and T. C. Lubensky, Phys. Rev. Lett. **104**, 085504 (2010).
[6] R. C. Picu, Soft Matter **7**, 6768 (2011).
[7] E. v. d. Giessen, Nat. Phys. **7**, 923 (2011).
[8] C. P. Broedersz, X. Mao, T. C. Lubensky, and F. C. MacKintosh, Nat. Phys. **7**, 983 (2011).
[9] C. Calladine, Int. J. Solids Struct. **14**, 161 (1978).
[10] J. Paulose, B. G. Chen, and V. Vitelli, Nature Physics, doi:10.1038/nphys3185.
[11] R. Hutchinson and N. Fleck, J. Mech. Phys. Solids **54**, 756 (2006).
[12] A. S. Phani and N. A. Fleck, J. Appl. Mech. **75**, 021020 (2008).
[13] V. Vitelli, Proc. Natl. Acad. Sci. USA **109**, 12266 (2012).
[14] K. Sun, A. Souslov, X. Mao, and T. C. Lubensky, Proc. Natl. Acad. Sci. USA **109**, 12369 (2012).
[15] C. L. Kane and T. C. Lubensky, Nat. Phys. **10**, 39 (2014).
[16] D. Mead, J. Sound Vib. **190**, 495 (1996).
[17] R. Langley, N. Bardell, and H. Ruivo, J. Sound Vib. **207**, 521 (1997).
[18] C. Chesnais, C. Boutin, and S. Hans, J. Acoust. Soc. Am. **132**, 2873 (2012).
[19] M. I. Hussein, M. J. Leamy, and M. Ruzzene, Appl. Mech. Rev. **66**, 040802 (2014).
[20] M. Ruzzene, F. Scarpa, and F. Soranna, Smart Mater. Struct. **12**, 363 (2003).
[21] A. S. Phani, J. Woodhouse, and N. Fleck, J. Acoust. Soc. Am. **119**, 1995 (2006).
[22] A. Spadoni, M. Ruzzene, S. Gonella, and F. Scarpa, Wave Motion **46**, 435 (2009).
[23] P. Celli and S. Gonella, J. Appl. Phys. **115**, 103502 (2014).
[24] P. Martinsson and A. Movchan, Q. J. Mech. Appl. Math. **56**, 45 (2003).
[25] See Supplemental Material at http://link.aps.org/supplemental/10.1103/PhysRevB.91.020103 for details of numerical procedures and additional parametric studies.
[26] P. Wang, J. Shim, and K. Bertoldi, Phys. Rev. B **88**, 014304 (2013).
[27] P. Wang, F. Casadei, S. Shan, J. C. Weaver, and K. Bertoldi, Phys. Rev. Lett. **113**, 014301 (2014).
[28] G. Wang, X. Wen, J. Wen, L. Shao, and Y. Liu, Phys. Rev. Lett. **93**, 154302 (2004).
[29] D. J. Colquitt, I. S. Jones, N. V. Movchan, and A. B. Movchan, Proc. R. Soc. London, Ser. A **467**, 2874 (2011).
[30] Z. Liu, X. Zhang, Y. Mao, Y. Zhu, Z. Yang, C. Chan, and P. Sheng, Science **289**, 1734 (2000).
[31] Y. Wu, Y. Lai, and Z.-Q. Zhang, Phys. Rev. B **76**, 205313 (2007).
[32] Z. Liu, C. T. Chan, and P. Sheng, Phys. Rev. B **65**, 165116 (2002).
[33] Y. Lai, Y. Wu, P. Sheng, and Z. Zhang, Nat. Mater. **10**, 620 (2011).
[34] D. Yu, Y. Liu, H. Zhao, G. Wang, and J. Qiu, Phys. Rev. B **73**, 064301 (2006).
[35] D. Yu, Y. Liu, G. Wang, H. Zhao, and J. Qiu, J. Appl. Phys.s **100**, 124901 (2006).
[36] C. Yilmaz, G. M. Hulbert, and N. Kikuchi, Phys. Rev. B **76**, 054309 (2007).
[37] S. Gonella, A. C. To, and W. K. Liu, J. Mech. Phys. Solids **57**, 621 (2009).
[38] W. Liu, J.-W. Chen, and X.-Y. Su, Acta Mech. Sin. **28**, 659 (2012).
[39] L. Liu and M. I. Hussein, J. Appl. Mech. **79**, 011003 (2012).
[40] Y. Xiao, J. Wen, and X. Wen, Phys. Lett. A **376**, 1384 (2012).
[41] Z. Wang, P. Zhang, and Y. Zhang, Math. Probl. Eng. **2013**, 146975 (2013).
[42] L. Raghavan and A. S. Phani, J. Acoust. Soc. Am. **134**, 1950 (2013).
[43] E. Kim and J. Yang, J. Mech. Phys. Solids **71**, 33 (2014).
[44] C. P. Broedersz and F. C. MacKintosh, Rev. Mod. Phys. **86**, 995 (2014).

Supporting Information for
Shaking Maxwell's rule - Locally resonant bandgaps in periodic beam lattices by tuning their connectivity

Pai Wang,[1] Filippo Casadei,[1] Sung Hoon Kang,[1] and Katia Bertoldi[1,2,*]

[1]*School of Engineering and Applied Sciences, Harvard University, Cambridge, Massachusetts 02138, USA*
[2]*Kavli Institute, Harvard University, Cambridge, Massachusetts 02138, USA*

CALCULATION OF DISPERSION RELATIONS

Periodic lattices and unit cells

The propagation of elastic waves in beam lattices is investigated numerically by considering 2D periodic lattices of infinite extent and focusing on their unit cell (i.e. a repeating geometric unit). The unit cells used in this study are shown in Fig. S1. Note that for hexagonal (Fig. S1b) and rhombic (Fig. S1c) lattices, the unit cells used in the calculations are not the minimum repeating units. In both cases an enlarged rectangular unit cell is chosen to be able to investigate all topologically equivalent lattices (constructed by varying the angles between connected beams) using the same computational setup.

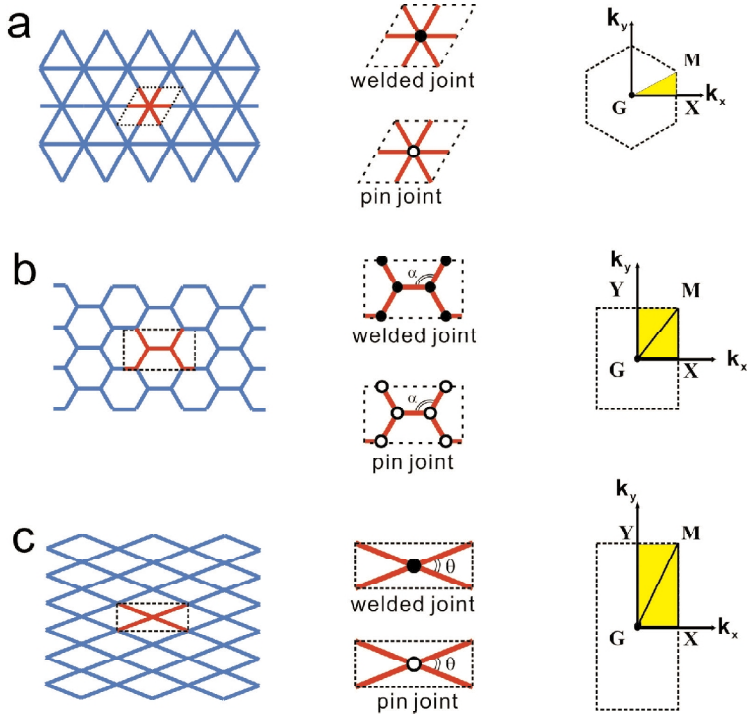

Figure S1: **Periodic lattices (left column) and their corresponding unit cells (central column), Brillioun zones (right column) and irreducible Brillioun zones (yellow shaded region) used in this study** for: **a,** Triangular lattice; **b,** Hexagonal lattice and its topologically-equivalent variants; and **c,** Square lattice and its topologically-equivalent variants (rhombic lattices).

Frequency-domain analyses and Brillioun zones

In order to obtain the dispersion relations of the propagating waves in the periodic lattices, frequency domain analyses are performed via finite element (FE) simulations using the commercial software ABAQUS/STANDARD. Preliminary calculations were performed using using both Euler-Bernoulli beam elements (ABAQUS element type B23) and Timoshenko beam elements (ABAQUS element type B21). Since the two sets of simulations yielded identical results, we chose to use Euler-Bernoulli beam elements for all the simulations. Bloch-wave [1] boundary conditions are applied to the boundaries of the unit cells:

$$\mathbf{u}(\mathbf{x}+\mathbf{r}) = \mathbf{u}(\mathbf{x})e^{i\,\mathbf{k}\cdot\mathbf{r}}. \tag{S1}$$

where $\mathbf{u}$, $\mathbf{x}$, $\mathbf{r}$ and $\mathbf{k}$ denote the degrees of freedom vector, position coordinates, spatial periodicity in the lattice configuration and bloch-wave vector, respectively. Note that for two-dimensional beam elements the vector $\mathbf{u}$ has three components, corresponding to two displacements (U1 and U2) and one rotation (UR3).

Focusing on the propagation of small-amplitude waves, we solve the linearized wave equation by using a perturbation method to obtain the dispersion relations $\omega = \omega(\mathbf{k})$. Due to the translational symmetry of the lattices, we only need to study $\omega(\mathbf{k})$ for $\mathbf{k}$ vectors in the *first Brillouin zone* [2, 3]. Moreover, this domain can be further reduced by taking advantage of rotational, reflectional and inversional symmetries of the Brillouin zone. This allows us to define the *irreducible Brillouin zone* (IBZ) [4], shown as the yellow triangle **GXM** in Fig. S1a and yellow rectangles **GXMY** in Figs. S1b and S1c. More details of mathematical formulation and numerical implementation are given in our previous publications [5, 6].

The phononic bandgaps are identified by checking all eigen-frequencies $\omega(\mathbf{k})$ for $\mathbf{k}$ vectors on the perimeter of the IBZ. The bandgaps (i.e. range in frequencies for which the propagation of waves is barred) are given by the frequency ranges within which no $\omega(\mathbf{k})$ exist. Numerically, a discrete set of $\mathbf{k}$ vectors on the IBZ perimeter needs to be chosen in the band-gap calculation. For the simulations presented in this paper, twenty uniformly-spaced points on each edge of the IBZ are used for the purpose of identifying band-gaps.

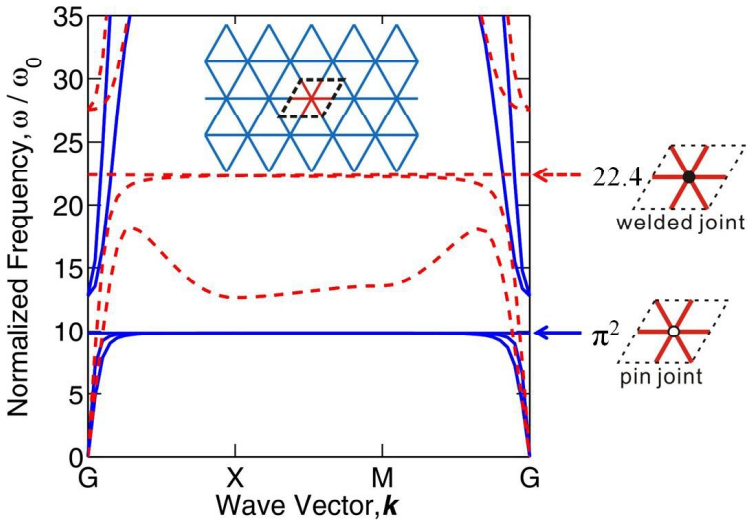

Figure S2: **Band structures of a triangular periodic beam lattices with welded (dashed red lines) and pin (continuous blue lines) joints.** The frequency bands in the plot are normalized by $\omega_0 = \omega_{pin}/\pi^2$.

ADDITIONAL RESULTS

Triangular lattice – comparison between pin and welded joints

The sound speed in the long-wavelength limit (i.e. the initial slope of the bands originated from **G**, the center of the *first Brillouin zone*) is directly correlated to the static homogenized stiffness of the structure. However, the slopes of the bands in Figs. 1a and 1b in the main article should not be compared directly for that purpose, since they are plotted using different normalization factors (i.e. the natural frequencies of a single beam with welded-welded and pin-pin boundary conditions, respectively). In fact, ω_{welded} and ω_{pin} differ by a factor of $22.4/(3.14)^2 = 2.27$. To facilitate the direct comparison of the band structure reported in Figs. 1a and 1b, we normalized the band structure for the case of both welded and pin junctions using the same factor, $\omega_0 = \omega_{pin}/\pi^2 = \omega_{welded}/22.4$. These results are reported in Fig. S2.

Hexagonal lattice and its topologically equivalent lattices with pin joints

In the main text we demonstrated that the dynamic response of the hexagonal lattice with welded joints is characterized by no locally resonant bandgap (see Fig. 2a). Furthermore, we showed that no band gap exists in periodic lattices with welded joints that are still characterized by $\bar{z} = 3$, but for which the angle between connected beams, α, varies from $2\pi/3$ to $\pi/3$ (see Figs. 2b, 2c and 2d).

Here, we report the band structures for the same lattices as those considered in Fig. 2 of the main text, but with pin joints. The results shown in Fig. S3 indicate that the flat-band resonant mode does not open a bandgap in this family of lattices even in the case of pin joints, confirming that the nature of the joints does not significantly affect the presence or absence of locally resonant bandgaps. However, it is important to note that the nature of the joints affects the static response of the system. In fact, the dispersion diagrams of the lattices with pin joints are characterized by a flat band at zero frequency [1] (indicated by the green lines in Fig. S3). This flat band at $\omega = 0$ corresponds to a "floppy" [8–12] or "soft " [13, 14] mode predicted by the Maxwell's Rule [7] and describes the *ground state* behavior of the lattice. Essentially, the existence of these zero-energy modes indicates that the lattice is not stable in a static sense and will collapse under infinitesimal perturbations. On the other hand, the full dispersion relation, including the "elevated flat bands" at $\omega/\omega_{pin} = 1$, defines the *excited state* response of the lattice under finite-energy dynamic loading. Interestingly, our results indicate that, differently from the ground state behavior, the excited state behavior of the lattices is not significantly affected by the nature of the joints.

[1] Note that such zero-frequency band is not present in the dispersion relation of a triangular lattice with pin joints (see Fig. 1b of the main text), since in that case the network is stable according to Maxwell's Rule [7].

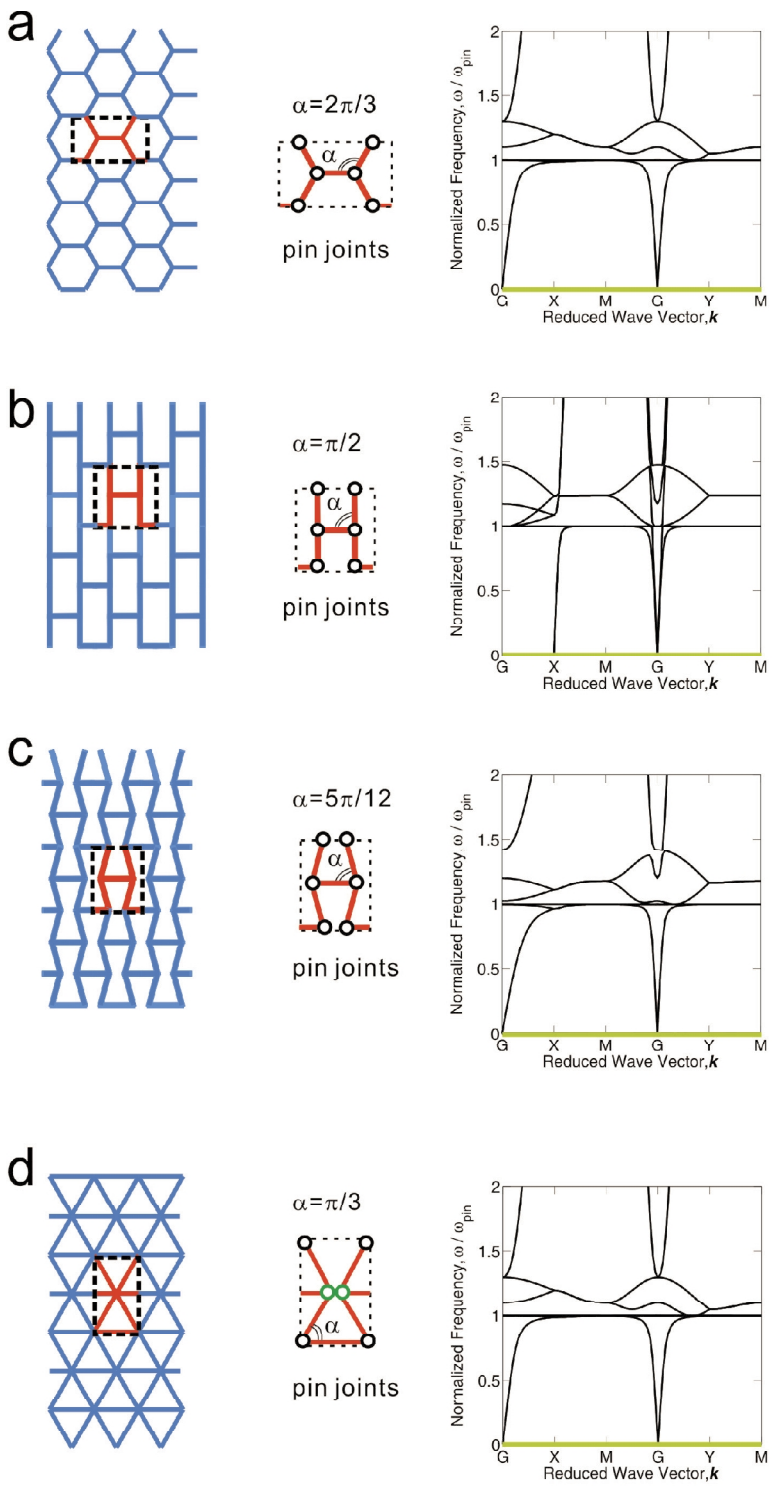

Figure S3: **Band structures of periodic lattices with $\bar{z} = 3$ and pin joints.** The lattice structures and unit cells used in the calculations are shown on the left. **a,** Hexagonal lattice ($\alpha = 2\pi/3$); **b,** Topologically equivalent lattice with $\alpha = \pi/2$; **c,** Topologically equivalent lattice with $\alpha = 5\pi/12$; and **d,** Topologically equivalent with $\alpha = \pi/3$. Note that the arrangement of the beams in **d** is the same as in the triangular lattice, but the connectivity is still $\bar{z} = 3$. In fact, although for clarity the green-colored joints are drawn separately in the unit cell of **d**, they are positioned at the same spatial location. No locally resonant bandgap is found for any of the configurations. The zero-frequency floppy modes are highlighted as green lines. Results for the same lattices with welded joints are provided in the main text.

Finally, it is worth noting that the band structures of a periodic lattices with $\bar{z} = 3$ and $\alpha = 2\pi/3$ (i.e. hexagonal lattice, see Fig. S3a) and $\alpha = \pi/3$ (see Fig. S3d) are identical. In fact, our numerical calculations show that for any β in the range $[0, \pi/2]$ the band structure of a periodic lattice with $\alpha = \pi/2 + \beta$ is the same as that of a lattice with $\alpha = \pi/2 - \beta$. More examples highlighting this symmetry are provided in Fig. S4.

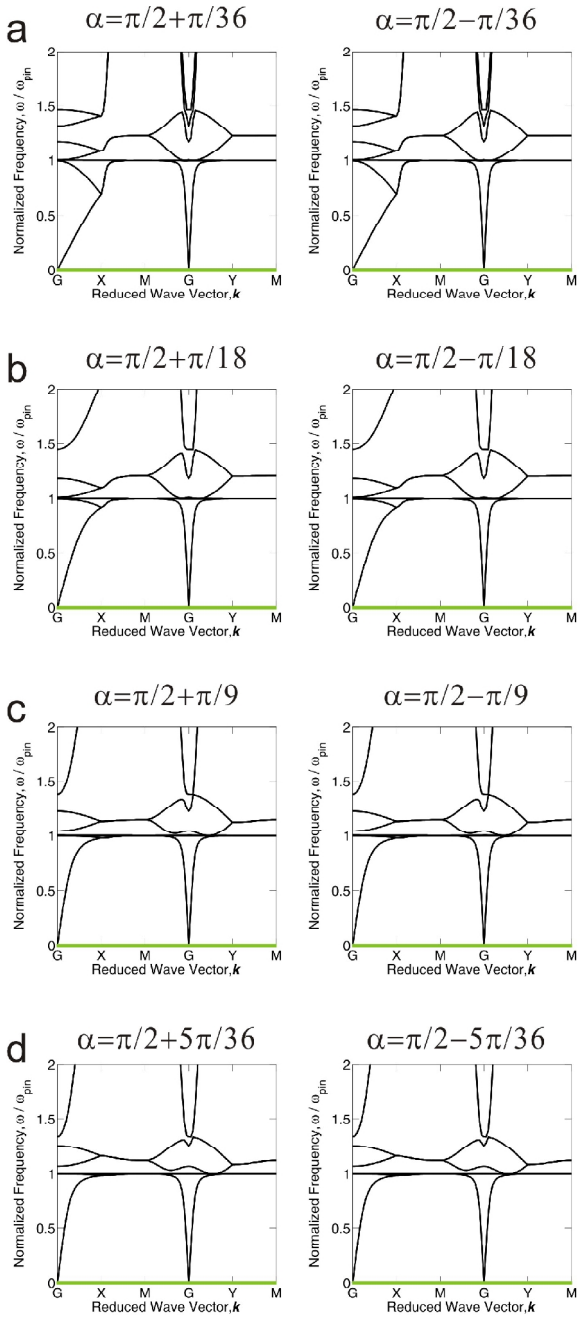

Figure S4: **Symmetry in the band structures of periodic lattices with $\bar{z} = 3$ and pin joints.** All results are for pin-jointed lattices that are topologically equivalent to the hexagonal lattice. Each row shows the dispersion relations for lattices with $\alpha = \pi/2 + \beta$ (left column) and $\alpha = \pi/2 - \beta$ (right column). In particular, we report results for with **a,** $\beta = \pi/36$; **b,** $\beta = \pi/18$; **c,** $\beta = \pi/9$; and **d,** $\beta = 5\pi/36$. The zero-frequency floppy modes are highlighted as green lines.

Periodic lattices with $3 \leq \bar{z} \leq 6$

To better understand the role of the coordination number on the formation of locally resonant bandgaps, we investigated the dynamic response of several periodic beam lattices with average connectivity $3 \leq \bar{z} \leq 6$ comprising an array of triangles and hexagons [2]. While in Fig. 3-b of the main text we summarized the results by reporting the evolution of the width of the bandgap $\Delta\omega$ as a function of the coordination number $\bar{z}$, here we show the dispersion relations for some of these lattices.

We note that, in general, these hybrid lattices do not possess rotational, reflectional and inversional symmetries and that only the time reversal symmetry [15] is guaranteed, yielding:

$$\omega(\mathbf{k}) = \omega(-\mathbf{k}). \tag{S2}$$

Therefore, Bloch vectors spanning half of the Brillouin zone need to be considered to construct the band structure. In practice, we calculate $\omega(\mathbf{k})$ for 21×21 different $\mathbf{k}$ vectors in half of the Brillouin zone and use the symmetry argument (Eq. (S2)) to map the results to the other half.

In Figs. S5, S6 and S7 we show the band structures for periodic lattices with $\bar{z} = 3.36$, $\bar{z} = 4.615$ and $\bar{z} = 5.143$, respectively. For $\bar{z} = 3.36$ no locally resonant bandgap is observed (see Fig. S5). Differently, for $\bar{z} = 3.36$ both configurations with (see Fig. S6-top) and without (see Fig. S6-bottom) locally resonant bandgap are found. Finally, for the case of high average connectivity such as $\bar{z} = 5.143$ all considered lattices possess a locally resonant bandgap (see Fig. S7).

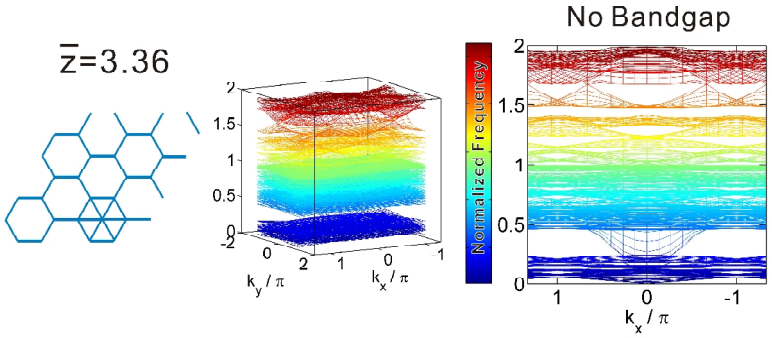

Figure S5: **Band structure for a periodic lattice with average connectivity $\bar{z} = 3.36$.**

[2] Note that the average connectivity can be easily calculated as the ratio between twice the total number of beams and the total number of nodes of the unit cell.

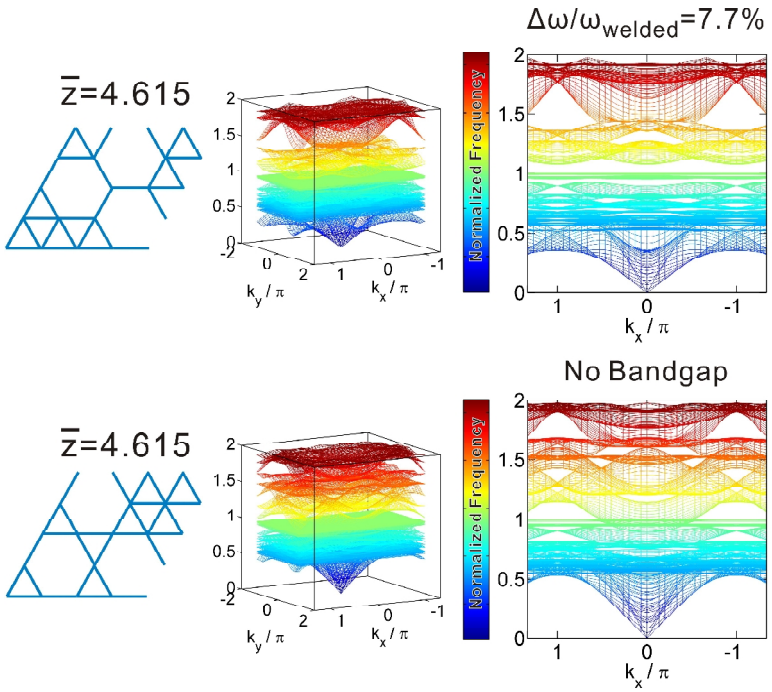

Figure S6: **Band structures for periodic lattices with average connectivity** $\bar{z} = 4.615$**.**

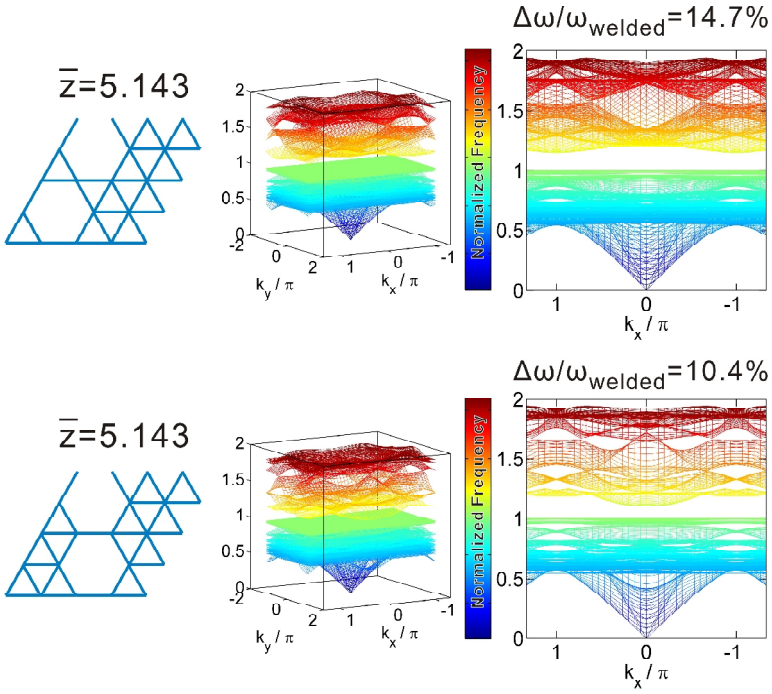

Figure S7: **Band structures for periodic lattices with average connectivity** $\bar{z} = 5.143$**.**

Rhombic lattices

In the main text we show that in rhombic lattices a locally resonant bandgap appears by progressively reducing the angle θ between the beams, regardless of the type of joints (see Fig. 4 of the main text).

Here, we show the band structures for rhombic lattices with $\theta = \pi/18$ (see Fig. S8-a), $\theta = \pi/6$ (see Fig. S8-b), $\theta = \pi/3$ (see Fig. S8-c) and $\theta = \pi/2$ (square lattice - see Fig. S8-d). Both lattices with welded and pin joints are considered. Note that for the cases of pin joints the lattices are characterized by a zero-frequency mode in the $\mathbf{G} - \mathbf{M}$ direction (see green lines in Fig. S8), since the structures are isostatic and can be infinitesimally deformed without incurring any energy cost.

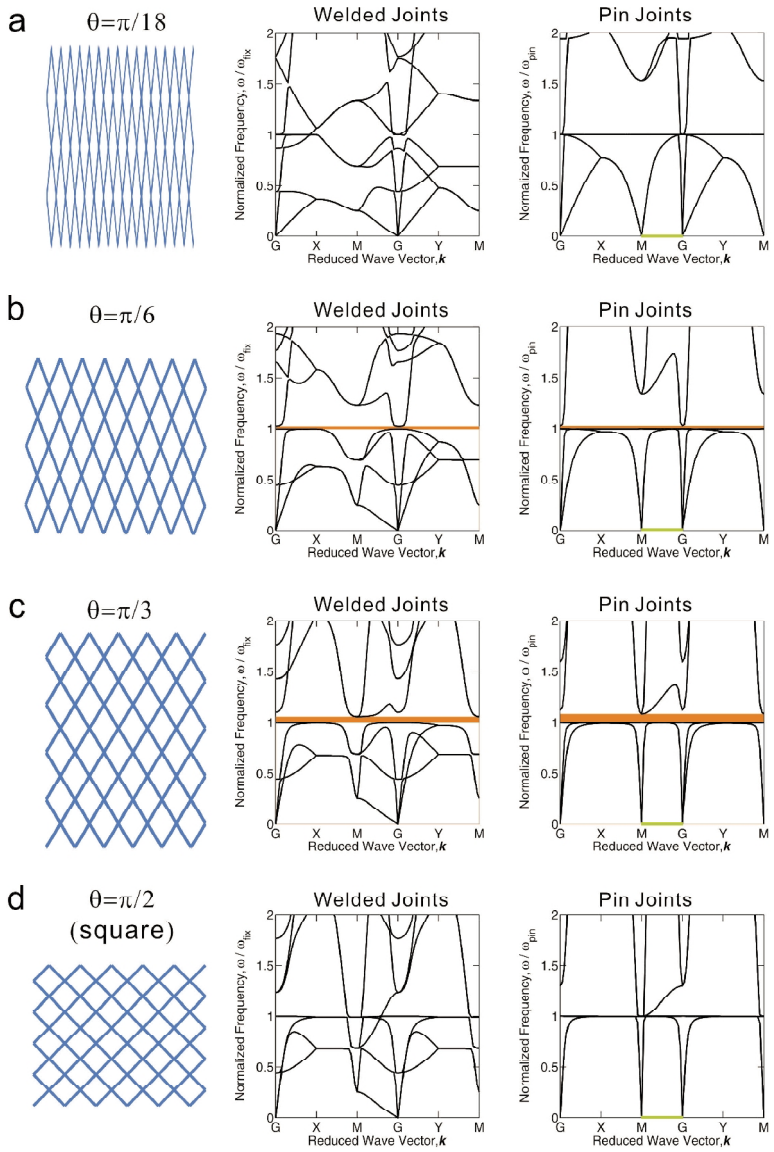

Figure S8: **Dispersion relations of rhombic lattices ($\bar{z} = 4$) with welded and pin joints.** The zero-frequency floppy modes in the **G-M** direction are highlighted as green lines. The bandgaps are highlighted as orange color-shaded area. **a,** $\theta = \pi/18$; **b,** $\theta = \pi/6$; **c,** $\theta = \pi/3$; and **d,** $\theta = \pi/2$ (square lattice)

* Corresponding author. bertoldi@seas.harvard.edu

[1] F. Bloch, Zeitschrift für physik **52**, 555 (1929).
[2] L. Brillouin, *Wave Propagation in Periodic Structures* (McGraw-Hill, 1946).
[3] L. Brillouin, *Wave Propagation and Group Velocity* (Academic Press, 1960).
[4] M. Maldovan and E. L. Thomas, *Periodic Materials and Interference lithography for Photonics, Phononics and Mechanics* (Wiley,-VCH, Weinheim, 2009).
[5] P. Wang, J. Shim, and K. Bertoldi, Phys. Rev. B **88**, 014304 (2013).
[6] P. Wang, F. Casadei, S. Shan, and K. Bertoldi, Phys. Rev. Lett. **111**, 111 (2014).
[7] J. C. Maxwell, Philos. Mag. Ser. 4 **27**, 294 (1864).
[8] A. J. Liu and S. R. Nagel, Annu. Rev. Condens. Matter Phys. **1**, 347 (2010).
[9] C. P. Broedersz, X. Mao, T. C. Lubensky, and F. C. MacKintosh, Nature Phys. **7**, 983C988 (2011).
[10] V. Vitelli, Proc. Natl. Acad. Sci. USA **109**, 12266 (2012).
[11] K. Sun, A. Souslov, X. Mao, and T. C. Lubensky, Proc. Natl. Acad. Sci. USA **109**, 12369 (2012).
[12] C. P. Broedersz and F. C. MacKintosh, arXiv p. 1404.4332v1 (2014).
[13] X. Mao, N. Xu, and T. C. Lubensky, Phys. Rev. Lett. **104**, 085504 (2010).
[14] R. C. Picu, Soft Matter **7**, 6768 (2011).
[15] J. D. Joannopoulos, S. G. Johnson, J. N. Winn, and R. D. Meade, *Photonic Crystals: Molding the Flow of Light (Second Edition)* (Princeton University Press, 2008), 2nd ed., ISBN 0691124566.